Optimized Price Based Frequency Regulation of Multi Area Restructured Power System with Wind Energy Conversion System

Shital M. Pujara[1] and Chetan. D. Kotwal[2]

[1]Research Scholar EE. Dept., Charusat University, Gujarat, India
[2]Professor & Head EE. Dept., SVIT, Vasad, Gujarat, India
smpujara4@yahoo.co.in, chetan.kotwal@gmail.com

Abstract: This paper describes the simulation of multi area multiple-units restructured power system with frequency regulation capability of the doubly fed induction generator (DFIGURE) through price based frequency-linked (PBFL) secondary control. Modified inertial control scheme responding proportionally to frequency deviations is used for DFIGURE to participate in frequency control of a mixed generation restructured system. Price based frequency-linked control acts as a supplementary control. The PBFL control is proportional to the unscheduled interchange (UI) based frequency linked pricing signal of availability based tariff (ABT) mechanism. The concept of contract participation factor (CPF) matrix is used to simulate the bilateral and contract violation transactions in the three area deregulated system. Integral gain of individual generating units are optimized through classical particle swarm optimization (PSO) technique, in order to have an optimal response of area frequencies, tie-lines power and power deviations of Gencos. MATLAB based simulations are carried out for three area deregulated power system to show the dynamic participation of doubly fed induction generator with frequency-linked pricing control in system frequency regulation. The various system responses have been studied to perceive the effects of the bilateral and contract violation transactions in deregulated market with consideration of different levels of wind penetration.

Index Terms: Doubly Fed Induction Generator; Price Based Frequency Linked Control; Availability Based Tariff; Particle Swarm Optimization; Restructured Power System.

1. Introduction

With the advent of deregulation in the electricity market, new organizations viz., generation companies (GENCOs), transmission companies (TRANSCOs), distribution companies (DISCOs), and independent system operators (ISOs) have emerged [1] which are responsible for maintaining the real-time generation-load balance so as to operate the system stably under highly competitive and distributed control environment. The modern restructured power sector consists of many power producing units of different types. The inertial and the dynamic characteristics of these new power generating sources differ from those of the conventional generating units in the past. As a result, load frequency control (LFC) have become more important and most profitable ancillary services in the restructured (deregulated) electricity market [2-3] and hence attract considerable attention from the system operators (SOs) and market players (MPs). There must be a perfect co-ordination among the new utilities to maintain the real time power balance, to minimize the tie-line power deviations, to facilitate various deregulated market transactions and to ensure the steady and secure operation of the power system.

A variety of controllers, based on advanced control techniques and special evolutionary algorithms have been proposed to study the LFC problem in the vertical integrated (regulated) interconnected power system to regain the frequency to its nominal value after any disturbance. Many of them have found it suitable in applying it with deregulated market scenario too and are discussed in the literature [4-11].

The frequency linked pricing scheme is also effective in frequency regulation and stabilizes the response much faster. This scheme encourages generators responding proportionally to frequency deviation or to a corresponding price signal sent out by the independent system operator (ISO) and helps to restore the system frequency back to nominal or very close to its

Received: April 24th, 2016. Accepted: March 25th, 2019
DOI: 10.15676/ijeei.2019.11.1.12

nominal value after any disturbances. The simulations conducted for load frequency control problem based on frequency linked pricing in a deregulated electricity market have been found in [12-15]. A fuzzy controller based frequency linked pricing scheme for competitive market structure is also suggested in [16]. Furthermore, unscheduled interchange based automated frequency linked pricing scheme, exclusively suitable to Indian regulated market scenario have been investigated by authors in literature [17-20]. After any disturbance, to bring back the frequency to its nominal value, the secondary frequency control should fully react with optimized gain of integral controller. Particle swarm optimization (PSO) technique is implemented to determine the optimal value of integral controllers in single area multi unit system through UI based frequency linked pricing mechanism [21]. Moreover fuzzy control based frequency linked pricing mechanism has been found in [22].

To reduce the dependency on fossil fuels, the electricity industry worldwide is diverting more towards the free and cleaner sources of energy to generate electricity because of their presumed infinite availability and absence of harmful emissions. Among various renewable energy resources, wind power is regarded to have the most promising technical and economic prospects with the greatest prospective to replace the conventional generation in electricity systems at present. With the large penetration of wind power into the power system, the grid frequency will be more susceptible to disturbances, as kinetic energy of wind generators will no longer be available to support the system frequency in the event of any disturbance. During any disturbance in the power system, the inertia of the wind turbine is effectively decoupled from the system and hence the useful inertia of the system 'seen' by the grid will be reduced, which results in increased rates of change of frequency. Moreover, restructuring of power system has created highly competitive and distributed control environment, and LFC becomes even more challenging when wind generators are also integrated into restructured power system. However, technological developments have made it possible for modern variable speed wind generators to participate in frequency control services. Considering this advancements, many researchers have developed a number of research schemes [23-27] for inertial support from the wind energy conversion units to reduce the adverse effects of load perturbation and contingency in deregulated power system. Moreover, the in-depth review study carried out by [28] exhibits the improved control capabilities of the variable speed wind turbine with the advancements in technology for frequency control services. Furthermore, a fuzzy controller based LFC problem in a hybrid deregulated system with the DFIGURE based wind turbine integrated into both the areas have been simulated and analyzed by author in [29] The coordinated control of the DFIGURE with frequency linked pricing scheme in a two area vertically integrated power system has been also discussed in [30].

The frequency linked pricing control scheme is one of the efficient and easy to implement scheme. But in very few cases only, it has been used to evaluate the LFC problem of today's power system.

The prime objective of this paper is to study the coordinated control of the DFIGURE in LFC of the three area multi-unit deregulated power system along with unscheduled interchange based frequency-linked pricing scheme. The paper emphasizes on the supremacy of LFC in mixed generation multi area deregulated power system through PBFL scheme compared to conventional frequency control scheme. Simulations are carried out for PBFL and conventional based secondary control alternatively with consideration of 10%, 20% and 30% of wind penetration levels to analyze various system responses of bilateral and contract violation transactions under restructured market scenario. More over PSO based optimized gain parameters of integral controllers of generators are used to obtain optimized system responses.

2. Restructured Power System

The earlier traditional electric industry was vertically integrated with all generation, transmission and distribution under its control with interlinking of the neighboring areas. The supply of power to the consumers was done at regulated rates. In the restructured (deregulated) environment, vertically integrated utilities no longer exist; instead it consists of different entities

viz.; generation companies (Gencos), transmission companies (Transcos), distribution companies (Discos), and independent system operator (ISO). In this new power system scenario, the engineering aspects of planning and operation are modified. As there are several Gencos and Discos in the restructured (deregulated) market, a Disco has the freedom to have a contract with any Genco for the transaction of power. Moreover, Gencos can sell their power to various Discos at competitive rates. Based on this information, three possible contracts are being practiced in restructured electricity market known as poolco, bilateral and contract violation. In poolco base contract, Gencos participate in load frequency control of their own areas only, whereas in a bilateral contract any Disco has the freedom to have a contract with any Genco in its own and other areas. Moreover, it may happen that a Disco violates a contract by demanding more power (contract violation) than that specified in the contract. This excess power is not contracted out to any Genco, but can be reflected as a local load of the area in addition with the contract demand. This un-contracted power of the area must be supplied by the Gencos in the same area as the Disco [6]. ISO is the sole responsible to supervise all these transactions.

A contract participation factor (CPF) matrix is used to express the contracts between various Gencos and Discos. This helps in easy visualization of various contracts made by Gencos and Discos. This information signals were absent in vertical integrated market scenario. CPF is a matrix with the number of rows equal to the number of Gencos and the number of columns equal to the number of Discos in the system.

The entry of the elements of CPF matrix (*cpfs*) corresponds to the fraction of the total load power contracted by Disco_j (j=1, 2, 3.....total no. Discos) from a Genco_i (i =1, 2, 3….total no. of Gencos). The sum of all the entries in a column in CPF matrix is unity (Donde etc al.2001; Bhatt et al. 2010). Also, the demand on Gencos is specified by

$$\Delta P_{gi} = \sum_{j=1}^{\text{total no of Discos}} cpf_{ij} * d_j \quad (1)$$

Moreover, along with contracted demand if any un-contracted demand arises, then the total demand on i^{th} Genco can be expressed as

$$\Delta P_{gi} = \sum_{j=1}^{\text{total no of Discos}} cpf_{ij} * d_j + Apf_i * d_{ucr} \quad (2)$$

$$\Delta P_{gi} = \sum_{j=1}^{\text{total no of Discos}} cpf_{ij} * d_j + GCE_i * d_{ucr} \quad (3)$$

Where d_j is the demand of j^{th} Disco; d_{ucr} is the total un-contracted demand of Discos from r^{th} area; Apf_i are the area control error participation factor of i^{th} Genco; and GCE_i is the generation control error signal of i^{th} generating unit.

Eq. (2) denotes total demand (generation power) on Gencos with conventional control in restructured market while Eq. (3) is used to calculate total demand on Gencos with PBFL control in restructured market. The scheduled steady state power flow on any tie line for restructured market is given as

$$\Delta P_{\text{tie r-m scheduled}} = \left\{ \begin{matrix} \text{Demand of Discos in area m from} \\ \text{Gencos in area r} \end{matrix} \right\} - \left\{ \begin{matrix} \text{Demand of Discos in area r from} \\ \text{Gencos in area m} \end{matrix} \right\} \quad (4)$$

$$\Delta P_{\text{tier-m,scheduled}} = \left\{ \sum_{\substack{i=\text{no.of gencos} \\ \text{of area r}}} \sum_{\substack{j=\text{no.of discos} \\ \text{of area m}}} cpf_{ij} * d_j \right\} - \left\{ \sum_{\substack{i=\text{no.of gencos} \\ \text{of area m}}} \sum_{\substack{j=\text{no.of discos} \\ \text{of area r}}} cpf_{ij} * d_j \right\} \quad (5)$$

3. DFIGURE-Based Wind Turbine Modeling

DFIGURE-based wind turbine can produce power with variable mechanical speed and extract kinetic energy to support the primary frequency regulation [23]. The active and reactive

power output of the DFIGURE system can be controlled as desired by the operator. Although the steady state active power delivered to the grid by the wind energy conversion system (WECS) depends on the wind speed, the power can be dynamically controlled to a certain extent by utilizing the stored mechanical energy. Upon the detection of a system network frequency disturbance, the extractable kinetic energy from the DFIGURE is used to supply more active power to the grid in order to reduce the initial fall of the frequency. It should be noted that this extracted active power of the DFIGURE, supports the grid frequency in the transient period only. When the system reaches a new steady state that is slightly less than nominal, the conventional generating units with integral controllers of load frequency control loop act to restore the frequency back to the nominal value. In this paper, the dynamic model represented in Figure.1 and discussed in [29-30] has been used for the study of frequency regulation with the essence of emulation control as given by [24].

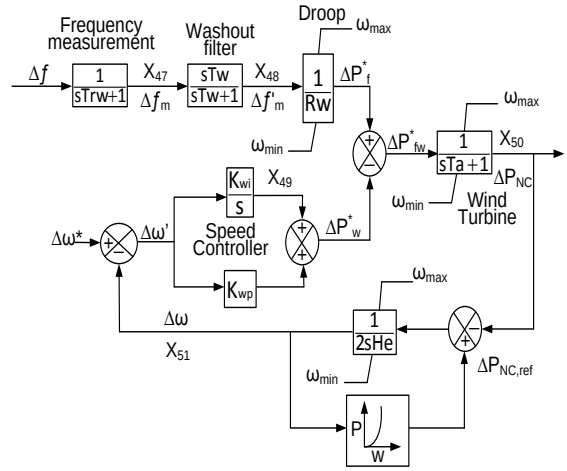

Figure 1. Frequency control model of DFIGURE-based wind turbine

The proposed inertial controller model is based on the conventional primary regulatory strategy only, but it is applied in a transient manner. The output from the proposed model is considered as an additional power reference to be tracked by the non-conventional equivalent machine controller. This reference power signal can be defined as:

$$\Delta P^*_f = \frac{1}{R_w}\Delta f'_m \quad (6)$$

Where R_w is the speed regulation of DFIGURE based wind turbine and $\Delta f'_m$ is measurement of change in frequency after a washout filter (high pass filter). This is done to avoid the permanent frequency deviation effect, as DFIGURE responds to frequency deviations during transient period only by releasing the stored kinetic energy in their rotating mass. A proportional-integral (PI) controller is used to recover the optimal rotor speed; after the period of transient frequency deviation is over. It is considered in the study that the DFIGURE recovers the optimal speed once the frequency transient is over. Hence a power set point ΔP^*_w, forcing the speed to track a desired speed reference, is defined as

$$\Delta P^*_w = K_{wp(\Delta\omega^* - \Delta\omega)} - K_{wi}\int(\Delta\omega^* - \Delta\omega)dt \quad (7)$$

Where $\Delta\omega^*$ and $\Delta\omega$ are incremental change in DFIGURE reference rotor speed and rotor speed respectively. While K_{wp} and K_{wi} are proportional and integral speed controller gain of DFIGURE based wind turbine respectively.
The total active power referenceΔP^*_{fw} is computed using Eq. (8).

$$\Delta P_{fw}^{*} = \Delta P_{f}^{*} - \Delta P_{w}^{*} \quad (8)$$

The active power injected by the DFIGURE is P_{NC} and is compared with reference active power output $P_{NC,ref}$ so as to obtain the maximum power output, by maintaining a reference rotor speed [25].

4. Price Based Frequency Linked Control

To deal with the problems associated with grid frequency control, a new three-part tariff scheme; availability based tariff (ABT) was introduced in India in the year 2000. The first component of ABT is fixed charge, second component is variable charge, and third component is unscheduled interchange (UI). This third component of ABT has frequency linked price and becomes effective, only when there are deviations in the scheduled power exchange.
The UI rates are decided by the central electricity regulation commission (CERC) and obtained from the frequency linked UI rate curve. The Frequency versus UI rate curve for the year 2014 is shown in Figure. 2.

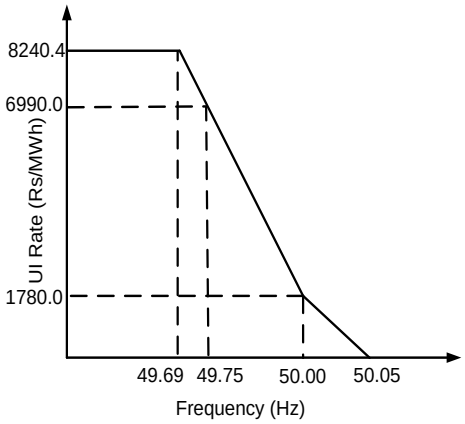

Figure 2. Frequency versus UI rate

The generating units respond to the UI price signal manually, leads to the delayed system response and an indistinct frequency profile. Whereas, price based frequency-linked (PBFL) mechanism for load frequency control ensures that generators respond to the UI price signal automatically in a desirable manner without any delay.

The author in [17] investigated load frequency control scheme based on UI price (price based frequency-linked control) to bring the frequency to a nominal value. According to this scheme, the primary control is similar to that of conventional frequency control, but the secondary control loop incorporates the frequency-linked UI price signal. However, this scheme suffers from a drawback that even when the load is as per the schedule; it results in unscheduled interchange among the generators at nominal frequency. Later, an author in [19] proposed the modified UI price based LFC scheme which overcomes the above mentioned drawback.

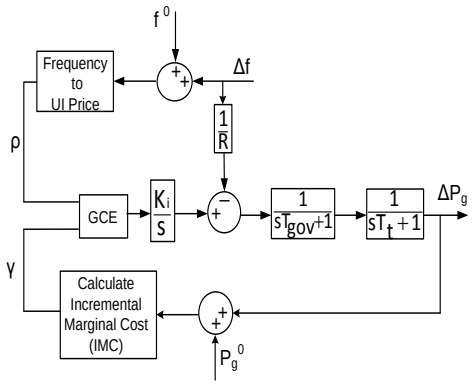

Figure 3. Modified price based load frequency control mechanism

The basic principle of modified UI based LFC is illustrated in Figure. 3. According to this scheme, each generator individually monitors the UI price ρ and compares with its incremental marginal cost γ and derives an error signal. For i^{th} generating unit incremental marginal cost is:

$$IMC_i = 2 * \left(\Delta P_{gi} + P_{gi}^0\right) * c_i + b_i \quad (9)$$

Where P_{gi}^0 is the initial generator scheduling; ΔP_{gi} is the change in generating power; and c_i and b_i are the cost co-efficient of the i^{th} Genco.

Now, this aforesaid error signal is fed to GCE logic block which in turn generates the output signal, known as generation control error (GCE) and subsequently it is sent to an integral controller. Further, this changes the setting of the governor which as a result changes to input power and hence readjust the frequency to its nominal value.

Wind, being a cheap and clean source of energy and at present is kept away from the ABT mechanism. To carry out the present work modified UI based LFC scheme shown in Figure. 3 and frequency versus UI rate curve of the year 2014 [31] shown in Figure. 2, are used. More details about GCE logic block and frequency to UI conversion can be found in article [19].

5. System Investigated

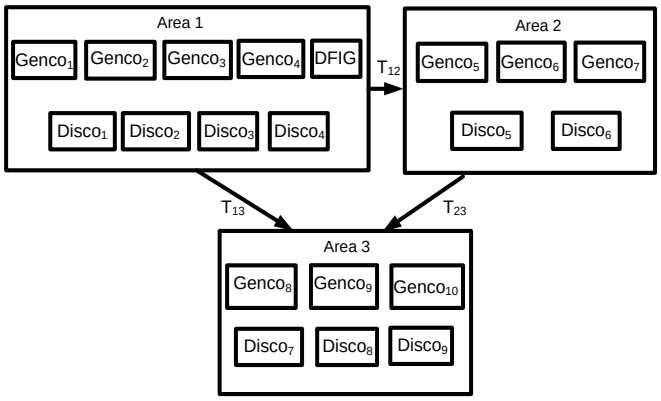

Figure 4. Schematic diagram of a three area system in restructured market with DFIGURE in area 1

As seen in Figure 4, the proposed system is a three area interconnected restructured power system with ten generators; nine discos; and with integration of DFIGURE based wind farm in area one. To obtain various simulation results, the secondary frequency regulation is either provided by a frequency-linked pricing mechanism or through conventional control mechanism in conventional thermal plants. After a load perturbation, DFIGURE and conventional thermal generating units respond to corresponding frequency deviations. The doubly fed induction

generator responds quickly during transients; whereas the UI price based frequency-linked secondary control or conventional secondary control of thermal generators take time to eliminate the frequency error.

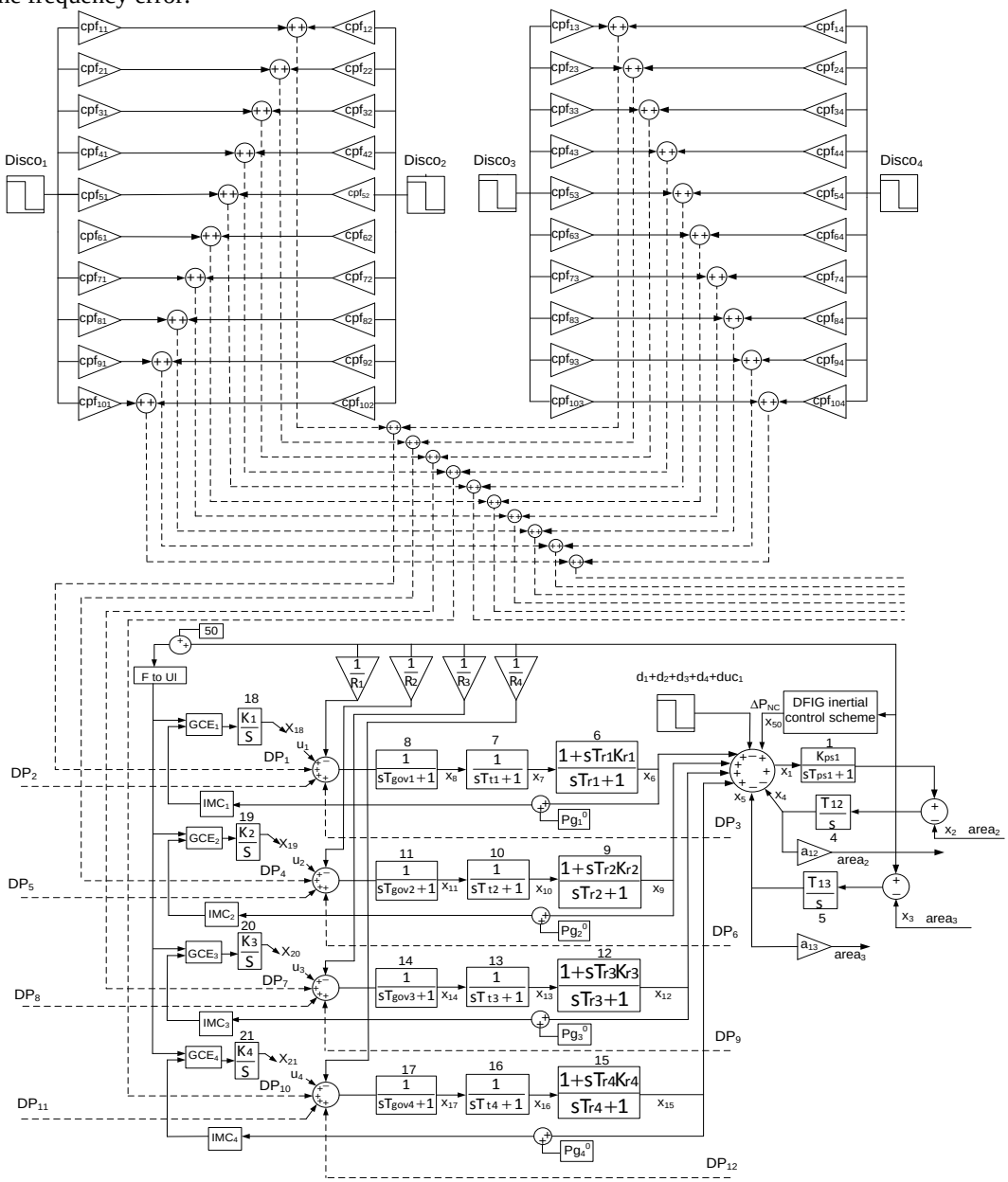

Figure 5. PBFL control block diagram in deregulated system with DFIGURE integration in first area

Figure 5 represents the block diagram of an implementation of PBFL control for generating units of the area one in three area deregulated system along with DFIGURE integration. Similarly, for generating units of area two and area three, PBFL control can be implemented. The complete system state space model for PBFL scheme with DFIGURE integration is of 51st order and mathematically written as:

$$\dot{x} = Ax + Bu + Fw + Py \tag{10}$$

Where, state variable matrix 'x':

$$x = \begin{bmatrix} x_1 = \Delta f_1 \\ x_2 = \Delta f_2 \\ x_3 = \Delta f_3 \\ x_4 = \Delta P_{tie12} \\ x_5 = \Delta P_{tie13} \\ x_6 = \Delta P_{tr1} \\ x_7 = \Delta P_{t1} \\ x_8 = \Delta P_{gov1} \\ x_9 = \Delta P_{tr2} \\ x_{10} = \Delta P_{t2} \\ x_{11} = \Delta P_{gov2} \\ x_{12} = \Delta P_{tr3} \\ x_{13} = \Delta P_{t3} \\ x_{14} = \Delta P_{gov3} \\ x_{15} = \Delta P_{tr4} \\ x_{16} = \Delta P_{t4} \\ x_{17} = \Delta P_{gov4} \\ x_{18} = u_1 \\ x_{19} = u_2 \\ x_{20} = u_3 \\ x_{21} = u_4 \\ x_{22} = \Delta P_{tr5} \\ x_{23} = \Delta P_{t5} \\ x_{24} = \Delta P_{gov4} \\ x_{25} = \Delta P_{tr6} \\ x_{26} = \Delta P_{t6} \\ x_{27} = \Delta P_{gov6} \\ x_{28} = \Delta P_{tr7} \\ x_{29} = \Delta P_{t7} \\ x_{30} = \Delta P_{gov7} \\ x_{31} = u_5 \\ x_{32} = u_6 \\ x_{33} = u_7 \\ x_{34} = \Delta P_{tr8} \\ x_{35} = \Delta P_{t8} \\ x_{36} = \Delta P_{gov8} \\ x_{37} = \Delta P_{tr9} \\ x_{38} = \Delta P_{t9} \\ x_{39} = \Delta P_{gov9} \\ x_{40} = \Delta P_{tr10} \\ x_{41} = \Delta P_{t10} \\ x_{42} = \Delta P_{gov10} \\ x_{43} = u_8 \\ x_{44} = u_9 \\ x_{45} = u_{10} \\ x_{46} = \Delta P_{tie23} \\ x_{47} = \Delta f_m \\ x_{48} = \Delta f'_m \\ x_{49} = k_{iw} * \int \Delta\omega' dt \\ x_{50} = \Delta P_{NC} \\ x_{51} = \Delta\omega \, dt \end{bmatrix} \tag{11}$$

Control input matrix 'u':

$$U=\begin{bmatrix} u_1 = k_{i1} * \int \Delta gce_1 dt \\ u_2 = k_{i2} * \int \Delta gce_2 dt \\ u_3 = k_{i3} * \int \Delta gce_3 dt \\ u_4 = k_{i14} * \int \Delta gce_4 dt \\ u_5 = k_{i5} * \int \Delta gce_5 dt \\ u_6 = k_{i6} * \int \Delta gce_6 dt \\ u_7 = k_{i7} * \int \Delta gce_7 dt \\ u_8 = k_{i8} * \int \Delta gce_8 dt \\ u_9 = k_{i9} * \int \Delta gce_9 dt \\ u_{10} = k_{i10} * \int \Delta gce_{10} dt \end{bmatrix} \quad (12)$$

Contracted disturbance input matrix 'w':

$$w = \begin{bmatrix} d_1 = \Delta P_{disco1} \\ d_2 = \Delta P_{disco2} \\ d_3 = \Delta P_{disco3} \\ d_4 = \Delta P_{disco4} \\ d_5 = \Delta P_{disco5} \\ d_6 = \Delta P_{disco6} \\ d_7 = \Delta P_{disco7} \\ d_8 = \Delta P_{disco8} \\ d_9 = \Delta P_{disco9} \end{bmatrix} \quad (13)$$

Un- contracted disturbance input matrix 'y':

$$y = \begin{bmatrix} d_{uc1} = \Delta P_{uc1} \\ d_{uc2} = \Delta P_{uc2} \\ d_{uc3} = \Delta P_{uc3} \end{bmatrix} \quad (14)$$

Where A, B, F, and P are the constant co–efficient matrix, which can be derived from system state equations. System state equations of first area are described in Appendix.

The aim of the LFC is to restore the frequency to its nominal value as quickly as possible and minimize the tie-line power flow oscillations between neighboring control areas after any load-generation disturbance. In order to satisfy the above requirements, gains of integral controllers in the LFC loops are required to be optimized. In the present work, an integral square error (ISE) criterion is used to minimize the objective function and define as performance index 'I':

$$I = \min\left\{\sum_{i=1}^{n} \Delta gce_i^2 + k_1 * \sum \Delta P^2{}_{\text{tie r-m,error}}\right\} * \Delta t \quad (15)$$

$$I = \min\left\{\sum_{1}^{\text{total no .of area}} \Delta f^2 + k_1 * \sum \Delta P^2{}_{\text{tie r-m,error}}\right\} * \Delta t \quad (16)$$

Where k_1 is weighting factor in the range of 10^5 multiply with $\sum \Delta P^2{}_{\text{tie r-m,error}}$ to make mutual competitive during optimization with $\sum_{i=1}^{n} \Delta gce_i^2$; Δt is small time interval during sample; $\Delta P_{\text{tie r-m error}}$ is incremental change in tie line error power; and Δgce_i the incremental change in generation control error of i^{th} Genco.

Eq. (15) is used to obtain the optimized gain values of integral controllers for DFIGURE with PBFL based LFC scheme, and Eq. (16) can be used to obtain the optimized gain values of integral controllers for DFIGURE with conventional LFC scheme. The objective function is minimized with the help of classical particle swarm optimization (PSO) based technique.

6. Particle Swarm Optimization

Particle swarm optimization (PSO) was first introduced by Kennedy and Eberhart (1995). It is a flexible, robust population-based search algorithm. It is developed through simulation of bird flocking in multidimensional space.

Suppose that the search space is N-dimensional, and the position of J^{th} particle of the population (swarm) is represented by an N- dimensional vector $S_J = (S_{J1}, S_{J2}, S_{J3} \ldots\ldots\ldots\ldots S_{JN})$. Each particle knows its best position so far. The best previous position visited by the J^{th} particle is denoted as $P_{bestJ} = \{P_{bestJ1}, P_{bestJ2}, P_{bestJ3} \ldots\ldots\ldots\ldots\ldots\ldots P_{bestJN}\}$. Moreover, each particle knows the best position so far in the group $G_{best} = \{G_{best1}, G_{best2}, G_{best3} \ldots\ldots\ldots\ldots G_{bestN}\}$ among $P_{bestJ1\ldots N.}$ The velocity (position change per generation) of the J^{th} particle is $V_J = \{V_{J1}, V_{J2}, V_{J3} \ldots\ldots V_{JN}\}$. In the swarm each particle's present position is realized by its previous position and present velocity information.

Mathematically, present velocities and present positions of the particles are determined by the following two Eqs.

$$V_J^{k+1} = W * V_J^k + C_1 * \text{Rand}_1 * \left(P_{bestJ} - S_J^k\right) + C_2 * \text{Rand}_2 * \left(G_{best} - S_J^k\right) \quad (17)$$

$$S_J^{k+1} = S_J^k + (K) * V_J^{k+1} \quad (18)$$

Where C_1 and C_2 are two positive constants and having the values between [0, 2.5]. Rand_1 and Rand_2 are two random numbers which have a stochastic influence on the velocity update and are uniformly distributed in [0, 1]; k is the iteration counter; and *K* is constriction factor, which insures the convergence of the particle swarm algorithm.
Value of *K* can be calculated as

$$K = \frac{2}{\left|2-\varphi-\sqrt{\varphi^2-4\varphi}\right|}, \text{W}here\ \varphi \geq 4 \quad (19)$$

Role of the inertia weight W is considered important for the PSO's convergence behavior. Suitable selection of inertia weight provides a balance between global and local explorations, thus requiring less iteration on an average to find a sufficiently optimal solution [32]. The inertia weight is determined by

$$W = W_{max} - \frac{W_{max} - W_{min}}{\text{Iter}_{max}} * \text{Iter} \quad (20)$$

Where W_{max} is the initial maximum weight; W_{min} is the final minimum weight; Iter_{max}, is the maximum iteration number; and Iter is the current iteration number. The performance of each particle is measured according to a minimum of fitness function, which is problem-dependent. In optimization problems, the fitness function is usually identical with the objective function under consideration.

Steps of PSO algorithm as implemented for optimization of gain K_i are:
Step I: Initialize real coded particles (K_i gains) of n_p population for each $K_{i.}$
Step II: Evaluate the objective function for all particles as given by Eqs. (15) or (16).
Step III: Search for individual minimum of objective function 'I' and its corresponding $P_{bestJ.}$
Step IV: Search for global minimum of objective function 'I' and its corresponding G_{best}.
Step V: Generate new population using Eqs. (17), (18), (19) and (20).
Step VI: Make a comparison with previous iteration data and update global best position.
Step VII: Update iteration counter and go to step II until the iteration counter reaches to its maximum value.

Table 1.

Integral Gains for co-ordinate DFIGURE and PBFL control	K_1	K_2	K_3	K_4	K_5	K_6	K_7	K_8	K_9	K_{10}
Bilateral with 10% wind penetration	3.0000 * 10^{-4}	1.3811 * 10^{-4}	3.0000 * 10^{-4}	3.0000 * 10^{-4}	1.7504 * 10^{-4}	3.0808 * 10^{-4}	2.0000 * 10^{-4}	1.0800 * 10^{-4}	9.0000 * 10^{-5}	1.0683 * 10^{-4}
Contract violation with 10% wind penetration	0.0136	0.0130	0.0067	0.0065	9.9780 * 10^{-5}	5.5761 * 10^{-5}	9.5884 * 10^{-5}	5.0446 * 10^{-5}	3.6069 * 10^{-5}	7.8350 * 10^{-5}
Bilateral with 20% wind penetration	2.7224 * 10^{-4}	1.7843 * 10^{-4}	1.000 * 10^{-4}	1.0000 * 10^{-4}	3.3731 * 10^{-4}	5.7970 * 10^{-4}	5.5305 * 10^{-4}	1.4741 * 10^{-4}	8.0000 * 10^{-5}	1.1878 * 10^{-4}
Contract violation with 20% wind penetration	0.0139	0.013	0.0067	0.0065	9.7568 * 10^{-5}	7.3873 * 10^{-5}	1.0000 * 10^{-4}	7.2845 *10^{-5}	1.2260 * 10^{-5}	5.000 * 10^{-5}
Bilateral with 30% wind penetration	2.8364 * 10^{-4}	1.7656 * 10^{-4}	* *10^{-4}	* *10^{-4}	2.4652 * 10^{-4}	3.7944 10^{-4}	3.4702 * 10^{-4}	1.7506 *10^{-4}	7.000 * 10^{-5}	1.4684 * 10^{-4}
Contract violation with 30% wind penetration	0.009	0.0086	0.0043	0.004	9.8179 * 10^{-5}	6.000 * 10^{-5}	8.4407 * 10^{-5}	1.2438 * 10^{-5}	4.4105 * 10^{-5}	6.0667 * 10^{-5}
Integral Gains for co-ordinate DFIGURE and Conventional Control	K_1				K_2			K_3		
Bilateral with 10% wind penetration	-0.869				-0.861			-0.852		
Contract violation with 10% wind penetration	-0.899				-0.875			-0.844		
Bilateral with 20% wind penetration	-0.9513				-0.9623			-0.950		
Contract violation with 20% wind penetration	-0.899				-0.861			-0.8543		
Bilateral with 30% wind penetration	-0.989				-0.98			-0.9865		
Contract violation with 30% wind penetration	-0.992				-0.990			-0.990		

Integral gains of three-area restructured power system with different wind penetration levels along with either PBFL or conventional control based schemes are optimized through classical PSO technique and compiled in Table 1.

7. Simulation Results and Discussion

Simulations are carried out for proposed restructured power system as shown in Figures. 4 and 5. Different possible contracts (transactions) under large load demands have been considered. To investigate the performance of multi area deregulated market with co-ordinate control of DFIGURE and PBFL control, in each transaction simulation results of various system responses viz.; frequency, actual tie-line power and change in Gencos power have been obtained and analyzed. Also, frequency excursion response of DFIGURE -based wind turbine with conventional control have been obtained and compared with price based frequency regulation scheme too. Moreover, in each transaction three different penetration levels (10%, 20%, and 30%) of wind energy are considered to investigate the impact of a DFIGURE in system operation. The level of wind penetration is defined as

$$W_r = \frac{\text{Wind generation}}{\text{Total generation in area}} * 100$$

Furthermore, it is assumed that wind speed remains constant during the simulation and that the DFIGURE-based wind turbine works at optimal speed with maximum power obtained from the wind. Also, to analyze the performance of DFIGURE-based wind turbine, active power and rotor speed responses are also obtained and compared with 10%, 20% and 30% wind penetration levels while participating for frequency control with price based frequency regulation scheme. d_1=0.1p.u.,d_2=0.1p.u.,d_3=0.05,p.u.,d_4=0.05p.u.,d_5=0.1p.u.,d_6=0.1p.u.,d_7=0.1p.u.,d_8=0.05 p.u.,d_9=0.05 p.u.

The un-contracted load in area one is expressed as duc_1= 0.058 p.u. and wind generation ΔP_{NC} = 10%, 20%, and 30%.

Test Case 1: Bilateral transaction

In this type of transaction, any Disco has the freedom to have a contract with any Genco in its own and other areas. Consider that all the Discos contract with the available Gencos for power as per the following contract participation factor (CPF) matrix.

$$CPF_b = \begin{bmatrix} 0.25 & 0.2 & 0.15 & 0.10 & 0.0 & 0.1 & 0.0 & 0.0 & 0.25 \\ 0.2 & 0.2 & 0.15 & 0.125 & 0.1 & 0.1 & 0.0 & 0.0 & 0.0 \\ 0.25 & 0.2 & 0.15 & 0.125 & 0.1 & 0.1 & 0.2 & 0.0 & 0.0 \\ 0.1 & 0.1 & 0.15 & 0.3 & 0.0 & 0.0 & 0.0 & 0.1 & 0.0 \\ 0.025 & 0.025 & 0.0 & 0.0 & 0.1 & 0.1 & 0.0 & 0.0 & 0.0 \\ 0.05 & 0.05 & 0.1 & 0.1 & 0.2 & 0.2 & 0.15 & 0.25 & 0.15 \\ 0.025 & 0.025 & 0.1 & 0.0 & 0.05 & 0.1 & 0.1 & 0.2 & 0.1 \\ 0.1 & 0.05 & 0.05 & 0.15 & 0.15 & 0.2 & 0.3 & 0.2 & 0.4 \\ 0.0 & 0.05 & 0.10 & 0.05 & 0.1 & 0.1 & 0.2 & 0.2 & 0.1 \\ 0.0 & 0.1 & 0.05 & 0.05 & 0.2 & 0.0 & 0.05 & 0.05 & 0.0 \end{bmatrix} \quad (22)$$

In the steady state, generation of Gencos must have to match the demand of the Discos which are in contract with it. This desired generation of Gencos is expressed in terms of cpf_s and the total demand of Discos, can be calculated using Eq. (1).

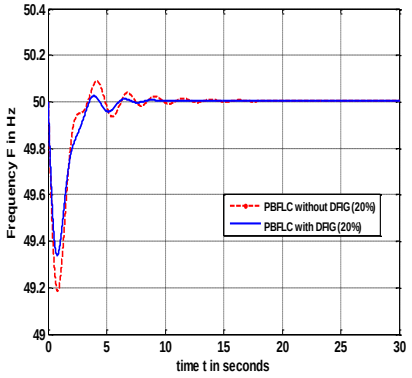
Frequency F in Hz
time t in seconds
PBFLC without DFIG (20%)
PBFLC with DFIG (20%)

(a)

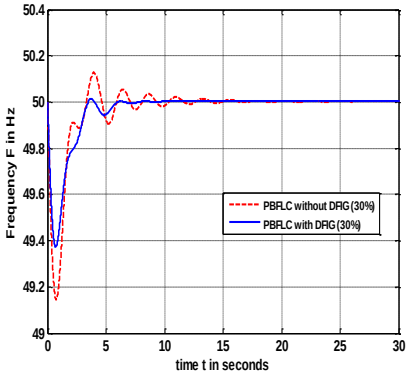
Frequency F in Hz
time t in seconds
PBFLC without DFIG (30%)
PBFLC with DFIG (30%)

(b)

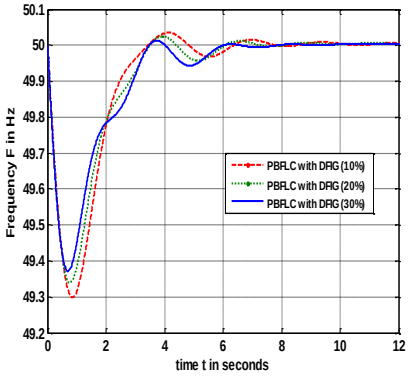
Frequency F in Hz
time t in seconds
PBFLC with DFIG (10%)
PBFLC with DFIG (20%)
PBFLC with DFIG (30%)

(c)

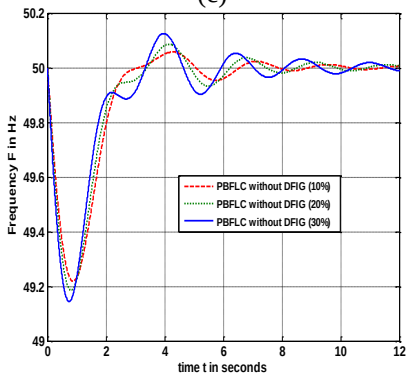
Frequency F in Hz
time t in seconds
PBFLC without DFIG (10%)
PBFLC without DFIG (20%)
PBFLC without DFIG (30%)

(d)

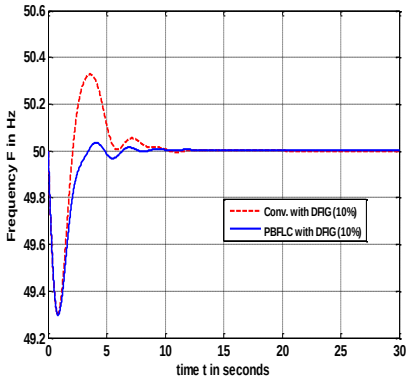

(e)

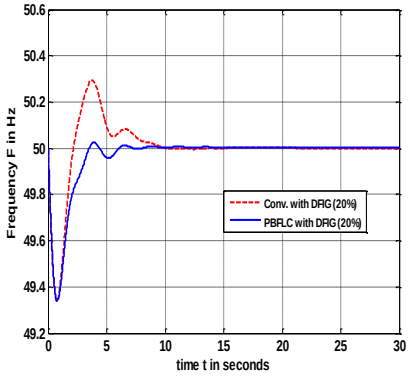

(f)

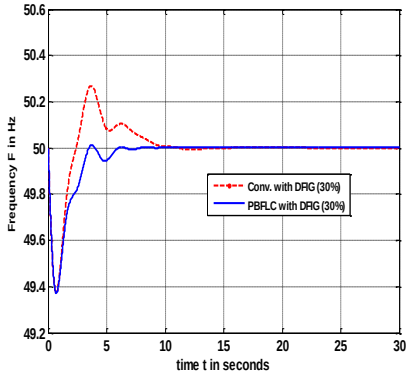

(g)

Figure. 6. Area one frequency curve with different wind penetration levels

When a DFIGURE participate in frequency regulation, it responds quickly and provides an active power support proportional to the frequency deviation and thus prevents the initial dip in frequency. Figures.6 (a-g), represent the frequency response of area one of proposed system with different wind penetration levels.

The behavior of the system frequency, for the cases with and without DFIGURE participation in frequency control through PBFL scheme are presented in Figures. 6 (a and b). The PBFL control responds to the UI price signal after comparing it with the incremental cost of the generating units as shown in Figure (5). The cost co-efficient of generating units are given in the Appendix. The incremental cost of Gencos in deregulated market is proportional to its contracted power requirement.

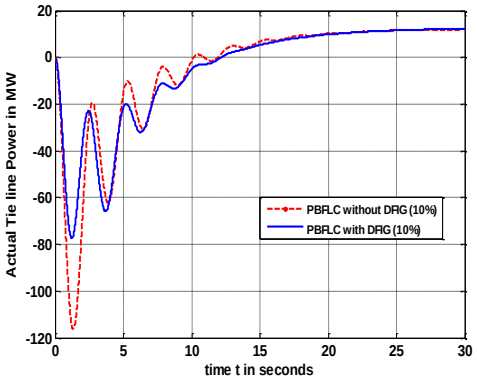
Actual Tie line Power in MW
time t in seconds
PBFLC without DFIG (10%)
PBFLC with DFIG (10%)

(a)

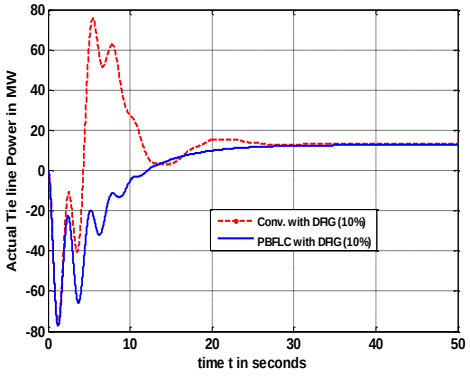
Actual Tie line Power in MW
time t in seconds
Conv. with DFIG (10%)
PBFLC with DFIG (10%)

(b)

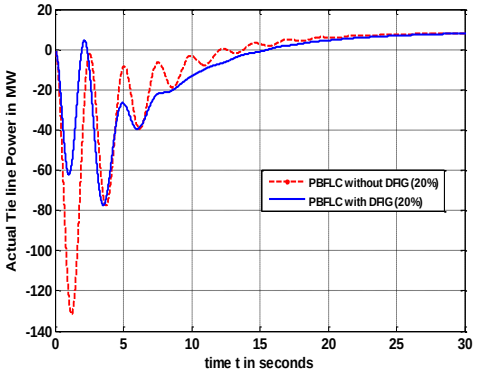
Actual Tie line Power in MW
time t in seconds
PBFLC without DFIG (20%)
PBFLC with DFIG (20%)

(c)

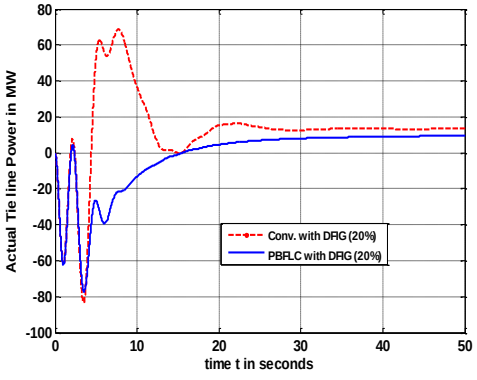
Actual Tie line Power in MW
time t in seconds
Conv. with DFIG (20%)
PBFLC with DFIG (20%)

(d)

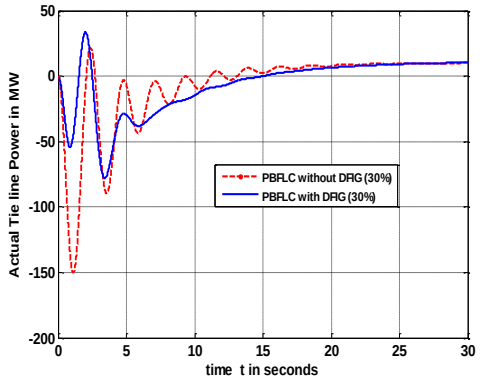

(e)

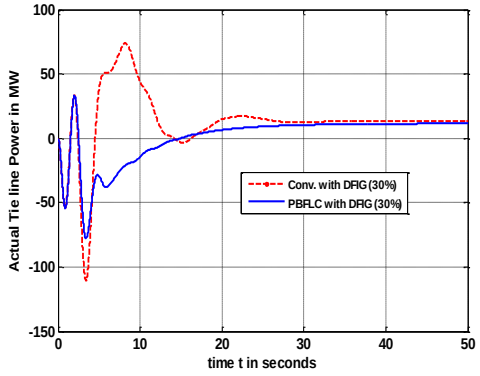

(f)

Figure. 7. Actual tie-line power flow of area one with different wind penetration levels

It is clearly observed that the frequency excursion is smaller when the DFIGURE are participating in the grid frequency control through PBFL control. Also, with frequency support from DFIGURE, if wind penetration increases; frequency excursion further reduces as depicted in Figure.6 (c). This improvement in the frequency response with inertial support from the DFIGURE system with an increased penetration level confirms the active participation of DFIGURE based wind turbine in system frequency regulation with PBFL control. Moreover, Figure.6 (d) validates that, when the DFIGURE based wind energy conversion system does not participate in the frequency regulation and as the wind penetration level increases; frequency excursion also increases along with PBFL control. Thus, aforementioned analysis substantiates the coordinated control of DFIGURE with thermal plants operated through PBFL scheme in multi area deregulated market. In Figures. 6(a-c) the comparison of frequency excursion curves of PBFL and conventional control scheme for bilateral contract with different wind penetration levels are shown. It can be observed from Figures. 6 (e-g) that for a different penetration level of wind, there is a drastic reduction in initial upper peak of frequency deviation, when a DFIGURE provides frequency support through PBFL control scheme as compared to the conventional control scheme with frequency support from DFIGURE. Thus, the DFIGURE along with the PBFL based secondary control applied in conventional thermal plant gives superior frequency response by lowering the peak of overshoot and less settling time.

The existence of the DFIGURE along with frequency support in the system helps to reduce the tie-line oscillations between the two control areas. Simulation results shown in Figures 7 (a-c) represent the behavior of the actual tie-line power flow. These simulations are carried out for contracted bilateral demand of Discos for the cases where the DFIGURE is participating in frequency control and when it is not participating in such control through PBFL scheme applied on thermal generators. As can be observed from the Figures. 7(a-c), with PBFL scheme, the tie-

line power oscillations have decreased considerably for DFIGURE with frequency control support compared to DFIGURE with no frequency control support at different wind penetration levels. Also, tie-line power reaches to its specified value in steady-state with frequency-linked pricing control which confirms the satisfactory operation of PBFL control in deregulated multi area power system with frequency support from DFIGURE. Moreover, comparisons of tie-line power responses for a conventional frequency control and PBFL control with DFIGURE participating in frequency support are presented in Figures. 7(d-f). It can be observed from these plots that the initial upper oscillations are considerably reduced with PBFL control compared to conventional control with frequency support from DFIGURE. The PBFL control scheme works without tie-line bias control where control area concept is notional and also no perception like area control error (ACE). Therefore, PBFL control scheme is quite simple compared to conventional control scheme. Also, frequency signal can be accessible to any power system control area and hence implementation of PBFL control scheme is easier.

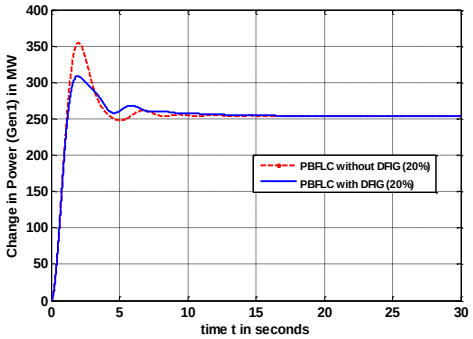

(a)

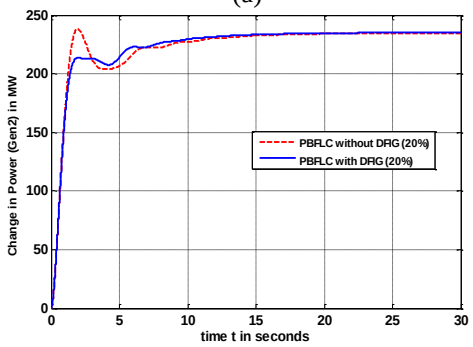

(b)

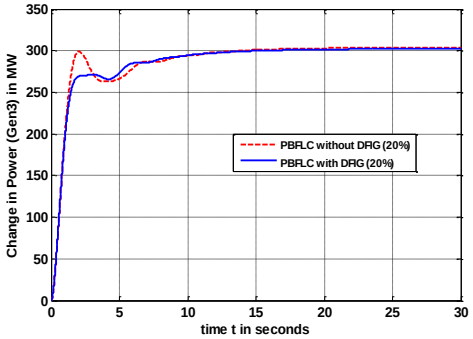

(c)

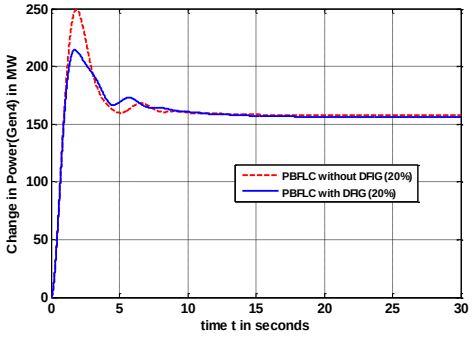

(d)

Figure 8. Change in generated power of Gencos of area one with 20% wind penetration level

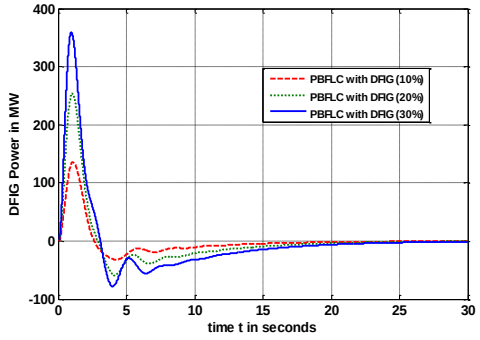

(a)

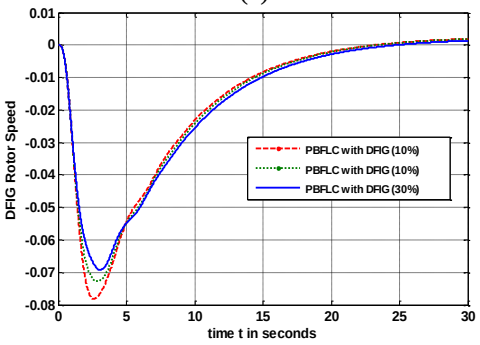

(b)

Figure 9. Change in DFIGURE active power and change in DFIGURE rotor speed with different wind penetration levels

Figures 8 (a-d), show the change in generation response of conventional generators following a step load change based on bilateral contract in area one with 20% wind penetration level. The step load change causes a significant fall in frequency, consequently conventional and DFIGURE both the type of generators would start increasing their generation to arrest the initial fall in frequency. The DFIGURE-based wind turbine response is instantaneous while that of a conventional generating unit is slower due to sluggish operation of governor control loop. It can be observed from the plots of the generating units of area one that, with the participation of DFIGURE, in frequency support through emulating inertia, the conventional generators in initial intervals are plagued less to regulate frequency. As discussed earlier, the DFIGURE provides frequency support during transients only, and hence the deviations in load are finally taken over by the conventional generators. Thus, with co-ordinate control of DFIGURE, conventional

Gencos attain the same generation level in steady state, but in initial periods, the generation of thermal units is less, as the DFIGURE releases kinetic energy instantly and provides active power support compared to no frequency support from DFIGURE. Also, change in Gencos power attain to its specified value in the steady state with frequency-linked pricing control which substantiates the acceptable operation of PBFL control in deregulated multi area power system with coordinated control of DFIGURE with frequency support.

Figures 9 (a and b), demonstrate the dynamic response of change in active power and change in rotor speed of the DFIGURE while participating in frequency control with PBFL control of thermal generators. To provide quick frequency support DFIGURE releases the kinetic energy stored in its rotating mass by decreasing its speed and thereby increasing its power output to contribute to frequency regulation. Thereafter, DFIGURE output for frequency support decreases, since the speed is no longer at the optimal value and power extracted from the wind is reduced. With the DFIGURE speed controller action the optimal speed is attained, the DFIGURE power output returns to its nominal value. It can be seen from the Figure. 9(a), that as wind penetration level increases, change in wind active power output also increases; which provides more inertial support from the DFIGURE. This behavior of the DFIGURE confirms that the higher the wind integration with frequency support control, lesser would be the frequency dip. It can also be revealed from Figure. 9 (b) that increased wind penetration level also increases inertia of the DFIGURE, so fall in rotor speed is lessened.

Test Case 2: Bilateral transaction with contract violation

MATLAB based simulations are carried out for a case of bilateral transaction with contract violation by introducing an additional load change of d_{uc1}= 0.058 p.u. in area one. This excess power is reflected as a local load of the area (un-contracted demand). The generators in the area one along with their predefined bilateral contract (as in the Test Case-1) respond to this un-contracted demand and their total demand can now be calculated either by using Eq. (2) or Eq. (3). The tie-line, power remains the same as in the Test Case-1.

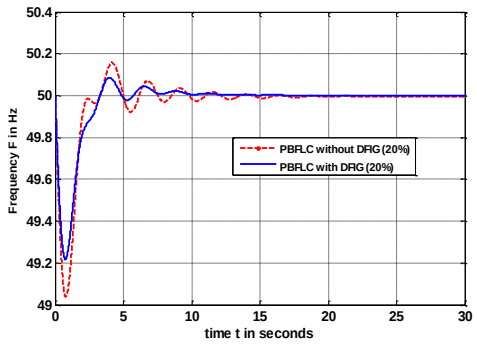

(a)

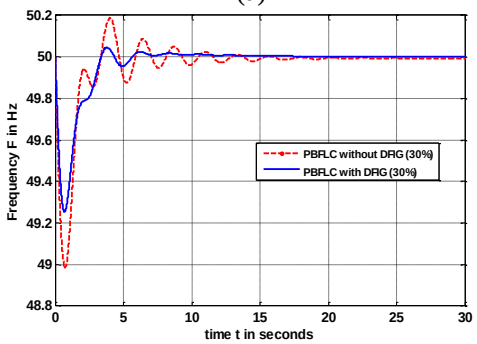

(b)

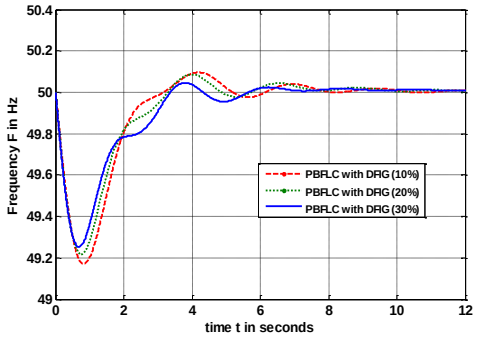
Frequency F in Hz
time t in seconds
PBFLC with DFIG (10%)
PBFLC with DFIG (20%)
PBFLC with DFIG (30%)

(c)

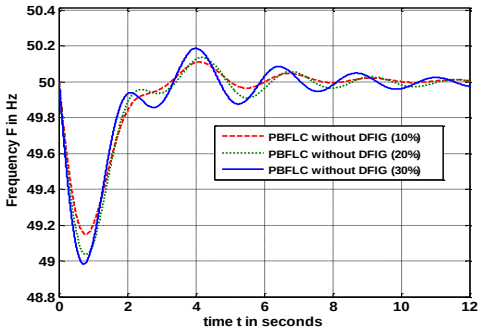
Frequency F in Hz
time t in seconds
PBFLC without DFIG (10%)
PBFLC without DFIG (20%)
PBFLC without DFIG (30%)

(d)

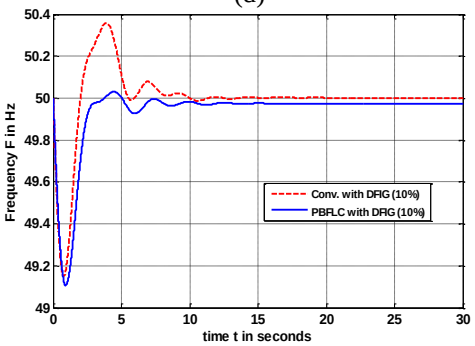
Frequency F in Hz
time t in seconds
Conv. with DFIG (10%)
PBFLC with DFIG (10%)

(e)

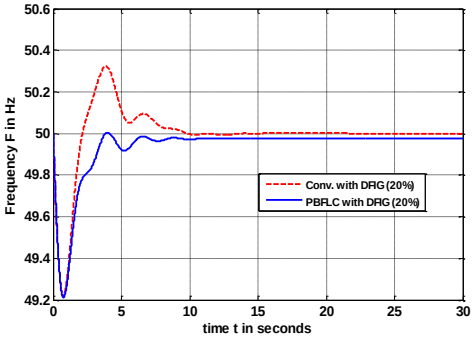
Frequency F in Hz
time t in seconds
Conv. with DFIG (20%)
PBFLC with DFIG (20%)

(f)

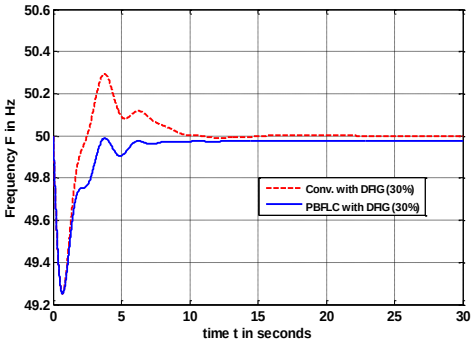

(g)

Figure 10. Area one frequency curve with different wind penetration levels

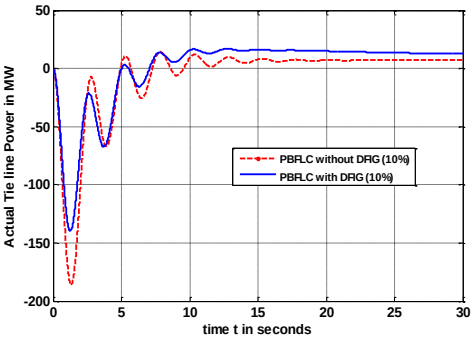

(a)

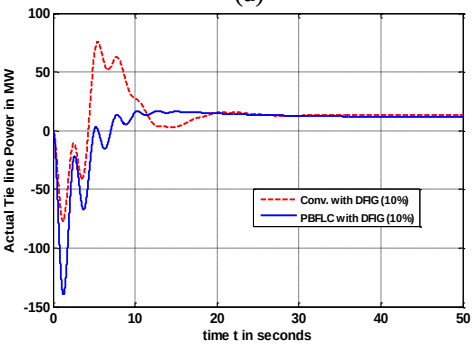

(b)

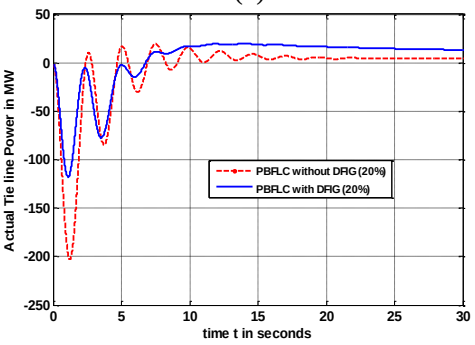

(c)

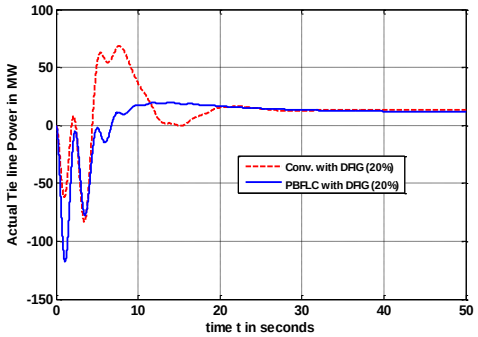

(d)

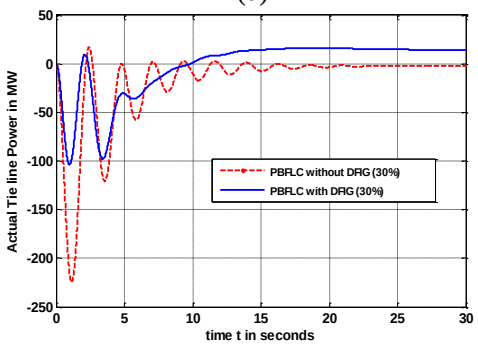

(e)

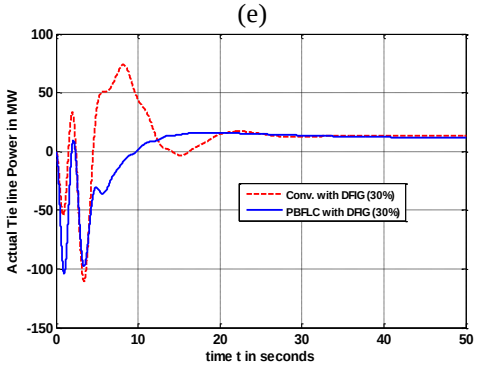

(f)

Figure. 11. Actual tie line power flow of area one with different wind penetration levels

Figures (10-13), shows the response of frequency, actual tie-line power flow, DFIGURE active power and rotor speed, and change in generation of area one generators. Observation of Figures. (10-12), reveal that the response of the system frequency, actual tie-line power, DFIGURE active power and rotor speed remain same that of the bilateral case, but initial fall or rise in each response is more immense compared to the bilateral transaction (Test Case- 1) system responses.

Figures 13 (a-d), exhibit that the generation of generators in area one is increased (more) compared to Test Case-1, as they have to meet extra un-contracted demand of same area Discos in addition to their contracted bilateral demand. This extra un-contracted demand is shared among the Gencos of same area as per their merit order dispatch, which is also one of the significant objective of UI based secondary control.

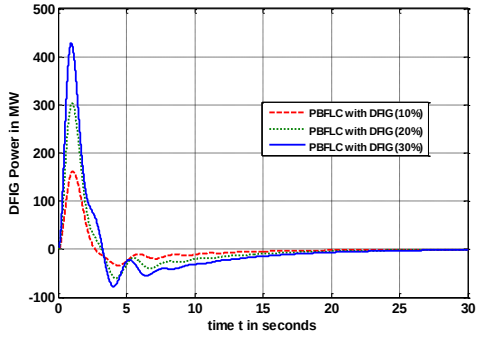

(a)

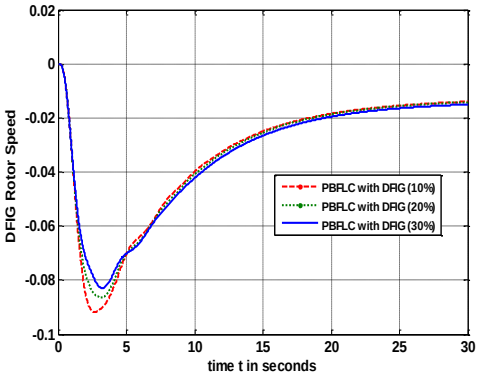

(b)

Figure. 12. Change in DFIGURE active power and change in DFIGURE rotor speed with different wind penetration levels

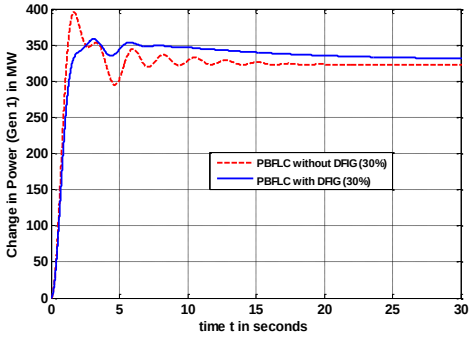

(a)

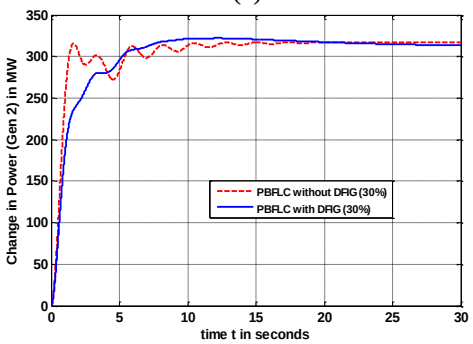

(b)

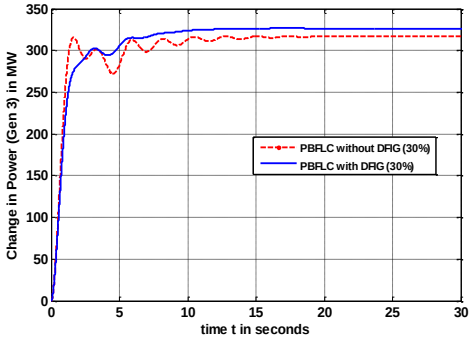

(c)

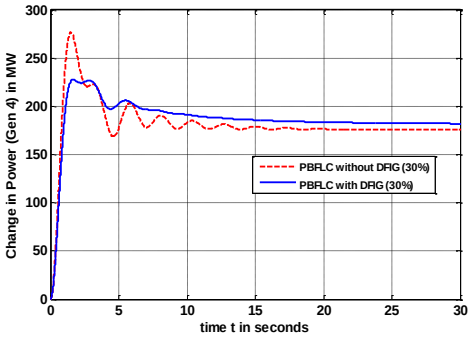

(d)

Figure 13. Change in generated power of Gencos of area one with 30% wind penetration level

8. Conclusions

This paper has analyzed the impact of DFIGURE based WECS in frequency control for three area deregulated power system with different wind penetration level using price based frequency control. The results obtained from MATLAB based simulation for bilateral and contract violation transactions under restructured electricity market, exhibit that, the price based frequency control collectively with DFIGURE works satisfactory in multi area system. PBFL control with frequency support from DFIGURE is superior compared to conventional frequency control to stabilize the system frequency and actual tie-lines power oscillations. In addition to this, an implementation of PSO optimized gain of integral controllers for individual generating unit improves the overall performance of the system. Also, frequency linked pricing control can be a greatly suitable choice to provide load frequency control in power-deficit countries like India to ensure the grid discipline in restructured electricity market scenario with mixed generation. Only by comparing frequency based pricing signal and marginal cost signal of generating unit the implementation of PBFL scheme will be easier compared to conventional LFC method.

9. References

[1]. R.D. Christie, and A. Bose, "Load Frequency Control Issues in Power System Operations after Deregulation," *IEEE Trans. on Power Systems*, Vol.11, No.3, pp.1191-1200, August 1996.

[2]. E. Rakhshani, and J. Sadeh, "Practical Viewpoints on Load Frequency Control Problem in a Deregulated Power System," *Energy Conversion and Management*, Vol.51, No.6, pp.1148-1156, June 2010.

[3]. S. M. Pujara, and C.D. Kotwal, "An Inclusive Review On Load Frequency Control in Deregulated Market," *International Journal on Electrical Engineering and Informatics*, Vol 8, No.3, pp. 594-610, July 2016.

[4]. A. Demiroren, and H.L. Zeynelgil, "GA Application to Optimization of AGC in Three-Area Power System After Deregulation," *Int. Journal of Electrical Power and Energy Systems*, Vol. 29, No.3, pp. 230-240, March 2007.
[5]. C.S. Rao, S.S. Nagaraju, and P.S. Raju, "Automatic Generation Control of TCPS Based Hydrothermal System under Open Scenario: A Fuzzy Logic Approach," *Int. Journal of Electrical Power and Energy System*, Vol.31, No.7-8, pp.315-322, September 2009.
[6]. P. Bhatt, R. Roy, and S.P. Ghoshal, "Optimized Multi Area AGC Simulation in Restructured Power Systems," *Electrical Power and Energy Systems*, Vol.32, No.4, pp.311-322, May 2010.
[7]. S. Bhongade, B. Tyagi, and H.O. Gupta, "Genetic Algorithm Based PID Controller for Frequency Regulation Ancillary Services," *International Journal of Engineering Science and Technology*, Vol. 2, No.12, pp. 6902-6908, January 2010.
[8]. P. G. Rana, R. Umrao, and D.K. Chaturvedi, "Automatic Generation Control with Polar Fuzzy Controller Considering Generation Rate Constraint in Deregulated Power System," *Proc. of Int. Conf. on Advances in Engineering, Science and Management*, pp. 610 - 615, March 2012.
[9]. K. Wadhwa, J. Raja, and S.K. Gupta, "BF Based Integral Controller for AGC of Multi Area Thermal System Under Deregulated Environment," *Proc. of IEEE Conf. on Power India*, pp.1- 6, December 2012.
[10]. P.K. Hota. and B. Mohanty," Automatic Generation Control of Multi-Source Power Generation Under Deregulated Environment," *International Journal of Electrical Power and Energy Systems*, Vol.75, pp. 205-214, February 2016.
[11]. M. Ma, C. Zhang, X. Liu. and and H Chen, "Distributed Model Predictive Load Frequency Control of the Multi-Area Power System After Deregulation," *IEEE Transactions on Industrial Electronics*, Vol. 64, No. 6, pp. 5129-5139, June 2017.
[12]. J. Kumar, K.H. Ng, and G. Sheble, "AGC Simulator for Price-Based Operation Part –I: A Model," *IEEE Transaction on Power Systems*, Vol.12, No.2, pp.527-532, May 1997.
[13]. J. Kumar, K.H. Ng, and G. Sheble, "AGC Simulator for Price Based Operation Part-II: Case Study Results," *IEEE Transaction on Power Systems*, Vol.12, No.2, pp.533-538, May 1997.
[14]. K. Bhattacharya, "Frequency Based Pricing as an Alternative to Frequency Regulation Ancillary Service," *Proc. of 11th National Power System Conference*, pp. 210-215, December 2010.
[15]. J. Zhong, and K. Bhattacharya, "Frequency Linked Pricing as an Instrument for Frequency Regulation in Deregulated Electricity Markets," *Proc. of IEEE Power Engineering Society Summer Meeting*, pp. 66-571, July 2003.
[16]. A. P. Fathima, and M. A. Khan, "Design of a New Market Structure and Robust Controller for The Frequency Regulation Services in the Deregulated Power System," *Electric Power Components and System*., Vol.36, pp.864–883, June 2008.
[17]. B. Tyagi, and S.C. Srivastava, "A Mathematical Framework for Frequency Linked Availability Based Tariff Mechanism in India," *Proc. of 13th National Power Systems Conf*., pp. 516-521, December 2004.
[18]. S. Chanana, and A. Kumar, "Proposal for a Real-Time Market Based on Indian Experience of Frequency Linked Prices," *Proc. of IEEE Conf. on Global Sustainable Energy Infrastructure*, pp.17-18, November 2008.
[19]. S. Chanana, and A. Kumar, "A Price Based Automatic Generation Control Using Unscheduled Interchange Price Signals in Indian Electricity System," *Int. Journal of Engineering, Science and Technology*, Vol.2, No. 2, pp. 23-30, April 2010.
[20]. N. Hassan, Ibrahim and S. Ahmed, "ABT Based Load Frequency Control of Interconnected Power System," *Electric Power Components and Systems*, Vol.44, No.8, pp.853-863, April 2016.

[21]. S. M. Pujara, and C.D. Kotwal, "Optimized Integral Gain Controllers for Price Based Frequency Regulation of Single Area Multi-Unit Power System," *International. Journal on Electrical Engineering and Informatics*, Vol.6, No. 2, pp.306-323, June 2014.
[22]. V. Murali and K. R. Sudha, "Price Based Fuzzy Automatic Generation Control for Indian Tariff System," *Energy System*, pp.1-16, January 2018.
[23]. G. Lalor, A. Mullane, and M. O'Malley, "Frequency Control and Wind Turbine Technologies," *IEEE Transaction on Power System*., Vol.20, No.4, pp.1905-1913, October 2005.
[24]. J. Morren, S. Haan, W. H. Kling, and J. A. Ferreira, "Wind Turbines Emulating Inertia and Supporting Primary Frequency Control," *IEEE Trans. on Power Syst*., Vol.21, No.1, pp.433-434, January 2006.
[25]. J. M. Mauricio, A. Marano, A. Gómez- Expósito, and J. L. M. Ramos, "Frequency Regulation Contribution Through Variable-Speed Wind Energy Conversion Systems," *IEEE Transaction on Power System*, Vol.24, No.1, pp.173–180, January 2009.
[26]. P. Bhatt, R. Roy, and S. P. Ghoshal, "Dynamic Participation of DFIGURE in Automatic Generation Control," *Renewable Energy*, Vol.36, pp.1203–1213, April 2011.
[27]. P. Bhatt, C. Long, J. Wu and B. Mehta, "Dynamic Participation of DFIGURE for Frequency Regulation in Electrical Power Systems', *Proc. of 9th International Conference on Applied Energy, U.K. Cardiff University*, pp. 2183-2188, 21-24 August 2017.
[28]. X. Yingcheng, and T. Nengling, "Review of contribution to frequency control through variable speed wind turbine," *Renewable Energy*, Vol.36, pp.1671–1677, June 2011.
[29]. Y.P. Verma, and A. Kumar, "Load Frequency Control in Deregulated Power System with Wind Integrated System Using Fuzzy Controller" *Frontier in Energy*, Vol.7, No.2, pp.245-254, December 2012.
[30]. Y.P. Verma, and A. Kumar, "Participation of Doubly Fed Induction Generator Based Wind Turbine in Frequency Regulation with Frequency-Linked Pricing," *Electric Power Components and Systems*, Vol. 40, No.14, pp. 1586-1604, October 2012.
[31]. Deviation Settlement Mechanism and Related Matters Regulations, www.cercind.gov.in. No. L-1/132/2013/CERC, New Delhi, India, January 2014.
[32]. J. Kennedy, and R.C. Eberhart, "Particle Swarm Optimization." Proc. of IEEE International Conference on Neural Network (Perth, Australia), *IEEE Service Center, Piscataway, NJ*, pp.1942- 1948,1995.
[33]. H. Bevrani, "Robust power system frequency control," Springer, 2009.

Appendix

Three Area System Data (T-T-T) [33]:

Area	1				2			3		
Generator unit	G1	G2	G3	G4	G5	G6	G7	G8	G9	G10
Rating(MW)	1200	600	800	800	600	1200	800	1400	600	600
H_i(s)	6	4	5	5	5	5	4	6	5	5
D_i (pu MW/Hz)	0.05	0.08	0.05	0.04	0.05	0.08	0.05	0.07	0.05	0.04
R_i (%)	3	3	3.2	2.7	2.7	2.6	2.5	2.8	3.0	3.0
T_{ti}	0.40	0.36	0.42	0.45	0.44	0.32	0.40	0.30	0.40	0.41
T_{govi}	0.3	0.2	0.07	0.1	0.3	0.2	0.15	0.15	0.15	0.2
T_{ri}	4.2	4.2	4.2	4.2	4.0	4.0	4.0	4.3	4.3	4.3
Kr_i	0.34	0.34	0.34	0.34	0.32	0.32	0.32	0.33	0.33	0.33
T_{mr} (pu MW/Hz)	T12=0.2				T21=0.2			T31=0.25		
	T13=0.25				T23=0.12			T32=0.12		
Cost co -efficient	Generators Cost Data									
b (Rs /MWh)	671	1450	732	488	610	871	700	800	1400	732
c (Rs/MW^2h)	1.0675	1.0675	3.8125	3.8125	1.50874	1.0675	1.525	1.05	1.0673	3.8125
	Initial Generation Scheduling Data									
PG_i^0 in (MW)	528.8	163.93	140.07	172.07	410.94	458.54	377.04	500	210.81	146

PSO Input Parameter for PBFL Control Scheme		DFIGURE Model Constants [29,30]	
No. of population	100	H_e (sec)	3.5
$Iter_{max}$	100	T_w (sec)	6.0
$C_1=C_2$	1.05	T_{rw}(sec)	0.1
W_{max}	0.8	T_a (sec)	0.2
W_{min}	0.3	K_{pw}	1.58
K	0.58	K_{wi}	0.1
		ω_{min} -ω_{max}(pu.)	0.8 -1.2
		V_w (met/sec)	7.5
		R_wH z/puMW)	3

Shital M. Pujara received her M.E. degree from S. P. University of V. V. Nagar, Anand, Gujarat, India. She has been a faculty member of Electrical Engineering Dept. in Sardar Vallabhbhai Patel Institute of Technology, Vasad, Gujarat, India since1997. At present she is pursuing her Ph.D. from CITC, Changa, Gujarat, India. Her areas of interests are inRestructured Power System,power System Economics, Simulation Techniques, and Evolutionary Algorithms.Email: smpujara4@yahoo.co.in, M- 9825707091.

Chetan D. Kotwal is a Professor at Department of Electrical Engineering, SVIT, Vasad, Gujarat, India. He received his B.E. and M.E. degrees from M.S. University of Baroda, Vadodara. He obtained his PhD. from Indian Institute of technology, Roorkee, India. His research interests are in Power Electronics applications to Power System, FACTS controllers and Power System Dynamics, Smart Grid, Power System Economics, Swarm Intelligence.Email: chetan.kotwal@gmail.com, M – 9909006055.